Dynamic relaxation of SU(2) lattice gauge theory in (3+1) dimensions

A. Jaster

Universität - GH Siegen, D-57068 Siegen, Germany

Abstract

We investigate the dynamic relaxation for SU(2) gauge theory at finite temperatures in $(3 + 1)$ dimensions. Using the Hybrid Monte Carlo algorithm, we examine the time dependence of the system in the short-time regime. Starting from the ordered state, the critical exponents β, ν and z are calculated from the power law behaviour of the Polyakov loop and the cumulant at or near the critical point. The results for the static exponents are in agreement with those obtained from simulations in equilibrium and those of the three-dimensional Ising model. The value for the dynamic critical exponent was determined with $z = 2.0(1)$.

Key words: Short-time dynamics; Non-equilibrium kinetics; Monte Carlo simulation; Lattice gauge theory

PACS: 11.15.Ha; 05.70.Jk; 02.70.Lq

1 Introduction

Traditionally, it was believed that universal scaling behaviour exists only in the long-time regime. However, recently Janssen, Schaub and Schmittmann [1] showed that far from equilibrium, in a macroscopic short-time regime of the dynamic evolution, there already emerges universal scaling behaviour in the O(N) vector model. They considered the relaxation process of a system quenched from a disordered state to the critical point and evolving with dynamics of model A (non-conserved order parameter and non-conserved energy [2]) and found that the magnetization undergoes an initial increase of the form $M(t) \sim t^{\theta}$, where θ is a new dynamic exponent and t denotes the time. This prediction was supported by a number of Monte Carlo (MC) investigations not only for O(N) vector models, but also for several other systems with a second-order or a Kosterlitz-Thouless phase transition [3]. These simulations

offer also a possibility to determine the conventional (static and dynamic) critical exponents [4–6] as well as the critical point [6]. This may eliminate critical slowing down, since the measurements are performed in the early part of the evolution.

In short-time critical dynamics exist two different time scales, the microscopic time scale t_{mic} and the macroscopic time scale t_{mac}. Universal behaviour emerges only after t_{mic}, the time during which the non-universal short wave behaviour is swept away. t_{mic} is independent of the linear space extension L and it is in general small compared to the macroscopic time scale, which is proportional L^z. After a time period of t_{mac} the correlation length is of the order of L and the system crosses over to the long-time universal behaviour.

First numerical simulations of the short-time dynamical relaxation at criticality started from a disordered initial state. However, dynamical scaling exists also for an ordered initial state. This is supported by a variety of MC investigations [3,7,8], but no analytical calculations exist for this situation. All static exponents as well as the critical point and the correlation length in the high temperature phase [9] can be also obtained with an ordered initial state.

Systematic numerical simulations of the short-time critical dynamics have been carried out mainly in two-dimensional systems [3,10,11,8]. Also, a first approach to lattice gauge theory was done for SU(2) gauge fields in $(2 + 1)$ dimensions [12]. The results strongly support that there exists a universal short-time scaling behaviour for the dynamic SU(2) lattice gauge theory. In this paper we investigate SU(2) gauge theory in $(3+1)$ dimensions. In contrast to the previous study in $(2+1)$ dimensions we start the dynamic evolution from an initial ordered state, i.e. with a magnetization of one at $t = 0$ ($m_0 = 1$). For the determination of the critical exponents, the dynamic relaxation process starting from an ordered state has been proven advantageous over that from an unordered initial state. This is a consequence of less prominent fluctuations for an ordered initial state. However, the new critical exponent θ can not been calculated if we start with $m_0 = 1$.

The dynamics of our system is given by the Hybrid Monte Carlo (HMC) algorithm [13]. Up to now mainly local algorithms such as the Metropolis or the heatbath algorithms have been used for the dynamic evolution. This is the first time that the HMC algorithm is studied in critical dynamic relaxation. The motivation for using the HMC algorithm is not only to enlarge the knowledge of short-time dynamics, but also the possibility to include fermions in future simulations. We examine the short-time behaviour of the order parameter and the cumulant at and in vicinity of the critical point. From the power law behaviour we extract the critical exponents β, η and z. The results are compared with those of simulations in equilibrium [14] and with simulations of the three-dimensional Ising model [7], since it is expected that both models

2

are in the same universality class [15].

In the next section we sketch the scaling analysis of the short-time critical dynamics. Sections 3 and 4 briefly describe the model and the updating algorithm. Numerical results are presented in Sec. 5. The last section contains the summary and conclusions.

2   Scaling relations

Using renormalization group methods, Janssen et al. have shown that even in macroscopically early stages of a relaxation process $O(N)$ vector models display universal behaviour [1]. They studied a system initially in a disordered state with vanishing or small magnetization ($m_0 \gtrsim 0$), suddenly quenched to the critical point and evolving with dynamics of model A, and derived the dynamic scaling form

$$M^{(k)}(t, \tau, L, m_0) = b^{-k\beta/\nu} M^{(k)}(b^{-z}t, b^{1/\nu}\tau, b^{-1}L, b^{x_0}m_0). \tag{1}$$

$M^{(k)}$ denotes the kth moment of the magnetization, t is the MC time of the dynamic relaxation, τ is the reduced coupling constant, b indicates a spatial rescaling factor and x_0 is a new independent exponent. For a sufficiently large lattice and small initial magnetization $m_0 \, t^{x_0/z}$ this leads to

$$M(t) \sim m_0 \, t^\theta, \quad \theta = (x_0 - \beta/\nu)/z \tag{2}$$

at the critical point $\tau = 0$.

Another important process is the dynamic relaxation from a completely ordered state. For an initial magnetization exactly at its fixed point $m_0 = 1$, a scaling form

$$M^{(k)}(t, \tau, L) = b^{-k\beta/\nu} M^{(k)}(b^{-z}t, b^{1/\nu}\tau, b^{-1}L) \tag{3}$$

is expected. The scaling form (3) looks the same as the dynamic scaling form in the long-time regime, however, it is now assumed already valid in the macroscopic short-time regime. The validity of the scaling form (3) in the short-time regime was verified with MC simulations for a number different systems [3].

Taking $b = t^{1/z}$ for the spatial rescaling factor in Eq. (3) with $k = 1$ leads for the magnetization to a power law behaviour

$$M(t) \sim t^{-c_1}, \quad c_1 = \frac{\beta}{\nu z} \tag{4}$$

3

at the critical point $\tau = 0$, if L is sufficiently large. For non-zero values of τ, the power law behaviour will be modified by the scaling function $M(1, t^{1/\nu z}\tau)$. This can be used for a determination of the critical point. Also, the critical exponent $1/(\nu z)$ [6] can be measured by taking the derivative with respect to τ

$$\partial_\tau \ln M(t, \tau)|_{\tau=0} \sim t^{c_{l1}}, \quad c_{l1} = \frac{1}{\nu z}, \tag{5}$$

while the dynamic critical exponent z can be determined from the behaviour of the cumulant

$$U(t) = \frac{M^{(2)}}{(M)^2} - 1. \tag{6}$$

Finite-size scaling shows that

$$U(t) \sim t^{c_U}, \quad c_U = \frac{d}{z}, \tag{7}$$

where d denotes the spatial dimension. Thus, the short-time behaviour of the dynamic relaxation starting from a completely ordered state is sufficient to determine all the critical exponents β, ν and z as well as the critical point. These measurements are usually better in quality than those starting from a disordered state.

3 SU(2) gauge theory at finite temperatures

The Wilson action for SU(2) gauge theory is given by

$$S = \frac{4}{g^2} \sum_P \left(1 - \frac{1}{2} \operatorname{Tr} U_P \right), \tag{8}$$

where U_P represents the usual plaquette term on the lattice. The number of lattice points in the space direction is L_s and in the time direction L_t. Thus, the volume and temperature are given by $V = L_s^3 L_t$ and $T = 1/L_t$, if we fix the lattice spacing a to unity. A point on the lattice has integer coordinates $x = (x_0, \boldsymbol{x}) = (x_0, x_1, x_2, x_3)$, which are in the range $0 \le x_0 < L_t$, $0 \le x_i < L_s$ ($i = 1, 2, 3$). A gauge field $U_{x,\mu}$ is assigned to the link pointing from point x to point $(x + \mu)$, where $\mu = 0, 1, 2, 3$ designates the four forward directions in space-time.

4

The order parameter (magnetization) of the system at some MC time t is the expectation value of the Polyakov loop

$$M(t) = \frac{1}{L_\text{s}^3} \sum_{\boldsymbol{x}} \langle L_{\boldsymbol{x}}(t) \rangle \,, \tag{9}$$

which is defined as the trace of ordered products of gauge field variables

$$L_{\boldsymbol{x}}(t) = \frac{1}{2} \text{Tr} \prod_{x_0=0}^{L_\text{t}-1} U_{(x_0, \boldsymbol{x}), 0}(t) \,. \tag{10}$$

The average is taken over independent measurements, i.e. independent random numbers. The deconfining phase transition of this model is of second order. The critical point for $L_\text{t} = 4$ was determined with $4/g_\text{c}^2 = 2.2989(1)$ for infinite large space extensions [14].

4   The HMC algorithm

Let us briefly sketch the HMC algorithm. In ordinary Metropolis or heatbath updating algorithms the new configuration is generated by sweeping over the whole system and changing locally the field variables q. In case of the HMC algorithm one uses molecular dynamics to generate the new configurations. One starts by introducing an additional, fictitious so-called molecular dynamics time t' and corresponding momenta p. The initial conjugate momenta p_i are generated from a Gaussian distribution of unit variance and zero mean. The fictitious time evolution of the fields and the momenta is now given by the following set of coupled first-order differential equations:

$$\dot{p}_i = -\frac{\partial \mathcal{H}}{\partial q_i}, \quad \dot{q}_i = p_i \,, \tag{11}$$

where the Hamiltonian is given by $\mathcal{H} = \sum_i p_i^2/2 + S[q]$. The time derivates are to be understood with respect to the fictitious time t'. The numerical integration of Eqs. (11) is performed by using a discretized version. In practice one uses a leap-frog integration scheme, using N_MD integration steps of size $\Delta t'$ in order to integrate from fictitious time 0 to some value $t' = N_\text{MD} \Delta t'$. The endpoint of these trajectories are considered as a trial new configuration, which is accepted or rejected according to the general Metropolis acceptance probability. The HMC algorithm is exact[1], i.e. systematic errors arising from

---

[1] The lack of reversibility coming from round-off errors in the numerical integration are discussed in Ref. [16].

finite time steps in the molecular dynamics are avoided by the accept/reject step. The algorithm is also ergodic due to the stochastic update of the initial momenta and fulfills the detailed balance condition, because of the reversibility of the leap-frog integration.

For SU(2) lattice gauge theory the equations of motion are

$$i\dot{H}_{x,\mu} = -\frac{4}{g^2}\left(U_{x,\mu}V_{x,\mu} - \text{h.c.}\right), \quad \dot{U}_{x,\mu} = iH_{x,\mu}U_{x,\mu},$$ (12)

where $H_{x,\mu}$ is the momentum conjugate to the field $U_{x,\mu}$ and takes the values in su(2), the Lie algebra of SU(2). $V_{x,\mu}$ denotes the staples around the link $U_{x,\mu}$, i.e. the incomplete plaquettes that arise in the differentiation[2]. The classical trajectories are computed using the leap-frog scheme, which consists of a sequence of intermediate points $(j = 0, \ldots, N_{\text{MD}}-1)$ of the following form

$$H_{x,\mu}(\Delta t'/2) = H_{x,\mu}(0) + \frac{\Delta t'}{2}\dot{H}_{x,\mu}(0),$$

$$U_{x,\mu}\left((j+1)\,\Delta t'\right) = \exp\left(i\,\Delta t' H_{x,\mu}\left(j\,\Delta t' + \frac{\Delta t'}{2}\right)\right)U_{x,\mu}(j\,\Delta t'),$$

$$H_{x,\mu}\left(j\,\Delta t' + \frac{\Delta t'}{2}\right) = H_{x,\mu}\left(j\,\Delta t' - \frac{\Delta t'}{2}\right) + \Delta t'\dot{H}_{x,\mu}(j\,\Delta t'),$$

$$H_{x,\mu}(t') = H_{x,\mu}\left(t' - \frac{\Delta t'}{2}\right) + \frac{\Delta t'}{2}\dot{H}_{x,\mu}(t').$$ (13)

The scheme is exact up to $\mathcal{O}(\Delta t'^2)$. In order to generate the desired Boltzmann distribution and to account for the discretization errors, the new configuration is only accepted with probability $P = \min\{1, \exp(-\Delta\mathcal{H})\}$, where $\Delta\mathcal{H} = \mathcal{H}(U(t'), H(t')) - \mathcal{H}(U(0), H(0))$ and the Hamiltonian is given by

$$\mathcal{H}[U, H] = \frac{1}{2}\sum_{x,\mu}\text{Tr}\left(H_{x,\mu}{}^2\right) + S[U].$$ (14)

5   Numerical results

We perform simulations with $L_{\text{t}} = 4$ and $L_{\text{s}} = 8$, 16 and 24 at the critical point $4/g_{\text{c}}{}^2 = 2.2989$ and in the neighbourhood[3] at $4/g^2 = 2.2689$ and 2.3289.

---

[2] Details of the HMC algorithm for gauge theory can be found in Ref. [17].
[3] For simulations in equilibrium these values would be considered to be far outside the critical region, especially for $L_{\text{s}} = 16$ and 24. However, these values are close enough to the critical point to calculate the derivative of the magnetization with

Starting from the ordered initial state, i.e. all link variables $U_{x,\mu}$ are set to unity, we measure the magnetization M and the cumulant U as a function of the MC time t. The system is updated with the HMC algorithm, where we fixed the length of the trajectory to $t' = 0.32$. A unit in the MC time t is defined as one global Metropolis step. Simulations are performed up to $t = 400$ global MC steps. The average is taken over $\mathcal{O}(1000)$ samples for $L_s = 8$, $\mathcal{O}(100)$ samples for $L_s = 16$ and $\mathcal{O}(10)$ samples for $L_s = 24$. Statistical errors are calculated by dividing the data into different subsamples. Systematic errors are estimated by the results of different system sizes and different time intervals, i.e. we examined the dependency of the critical exponents from the fitted interval $t = [t_{\min}, t_{\max}]$ and the space direction L_s. The quoted error is a sum of the statistical and systematic error.

In Fig. 1 we plot the time evolution of the magnetization at the critical point for different system sizes on a double logarithmic scale. Statistical errors are of the order of the distance between the curves. For $L_s = 16$ a trajectory of the HMC algorithm consists of 80 steps with $\Delta t' = 0.004$. To get comparable results for the other lattices ($L_s = 8, 24$), one can not perform simulations with the same parameters $(N_{\mathrm{MD}}, \Delta t')$ [4]. The reason is the global accept/reject step. The difference of the final and initial values of the Hamiltonian increases for larger lattices, so that using the same parameters would result in a lower acceptance rate. Therefore, we scale the step size with $\Delta t' \sim L_s^{-1}$ to get comparable acceptance rates. Since the trajectory length t' is constant, we have to scale $N_{\mathrm{MD}} \sim L_s$ so that the CPU time scales also with L_s. In all cases ($L_s = 8, 16, 24$) we get an acceptance rate of approximately 99%.

However, also if we scale the parameters in the way described there are large deviations for the different system sizes at small times. This might arise from statistical effects coming from the global accept/reject step. Especially for the largest lattice we have a small statistics and the effect of a global reject step at small times is high. Also, the acceptance rate (which is calculated by averaging over the 400 MC steps) for early times is relatively small. However, the results show that finite size effects coming from the finite space dimension are small up to $t = 400$, i.e. the influence of finite lattice size in Eq. (4) do not show up in the time interval used [5]. Therefore, $L_s = 16$ is large enough to avoid systematic errors from too small lattices.

Obviously, the magnetization which is shown in Fig. 1 can be described by a power law behaviour if we leave out the data for small times up to t_{mic}. Thus, the time interval shown is completly within the short-time regime. The

---

respect to τ in the short-time region.

[4] In case of the local Metropolis algorithm simulations of different system sizes can be simply performed with the same parameters.

[5] A system starts to show finite size effects after a time scale proportional L^z, which leads to deviations from the power law behaviour.

microscopic time scale during which the non-universal behaviour is swept away is about 40. The slope of the curve yields the value of the exponent $c_1 = \beta/\nu z$. The results of the different space dimensions, subsamples and time intervals lead to $c_1 = 0.248(5)$.

The critical exponent c_1 should be independent of the step size $\Delta t'$ and number of steps N_{MD} of the trajectory. However, a change of these parameters can lead to a different microscopic time scale t_{mic} and a change of the statistical errors. To examine the influence of the parameters $\Delta t'$ and N_{MD} we study the short-time critical dynamics of the magnetization with $\Delta t' = 0.002$ and $N_{\mathrm{MD}} = 160$ for $L_{\mathrm{s}} = 16$. The results are compared with the measurements using $\Delta t' = 0.004$ and $N_{\mathrm{MD}} = 80$ and are shown in Fig. 2. The acceptance rate changes from 98.7% for $N_{\mathrm{MD}} = 80$ to 99.7% for $N_{\mathrm{MD}} = 160$, while the CPU time increases by a factor of two. Although the changes for the acceptance rate are small, there are large deviations between both measurements at small times. Figure 2 shows that the microscopic time scale t_{mic} decreases for smaller $\Delta t'$. The difference between both simulations at larger times are negligible and the values for the critical exponent c_1 coincide within statistical errors.

To extract the critical exponent c_{l1}, we measure the magnetization as a function of time also below and above the critical point. The simulations are performed with $L_{\mathrm{s}} = 16$, $N_{\mathrm{MD}} = 80$ and $\Delta t' = 0.004$. The results are visualized on log-log scale in Fig. 3. These data are used to calculate the logarithmic derivative of the magnetization with respect to g_{c}. This is shown in Fig. 4. The slope provides $c_{l1} = 0.83(3)$, where the error of c_{l1} is dominated by systematic effects. In principle, one can also use the simulations to estimate the critical point. This is done by searching the best power law behaviour of $M(t)$ between the two values $4/g_1{}^2 = 2.2689$ and $4/g_2{}^2 = 2.3289$ as described in Ref. [6]. Namely, the best straight-line fit to curves obtained by quadratic interpolation for $g_1 > g > g_2$ is sought. However, our statistic is not good enough so that we do not perform this analysis.

The final step is to determine the critical exponent z. This is done by measuring the cumulant $U(t)$ and extracting the exponent d/z. Our simulations yield $z = 2.0(1)$. Thus we get $\nu = 0.60(5)$ and $\beta = 0.30(2)$. These results are in agreement (within statistical errors) with those obtained from simulations in equilibrium [14], which are $\nu = 0.630(11)$ and $\beta = 0.328(6)$. Also, the data coincide with those of the three-dimensional Ising model [7]. Performing similar measurements (but using the Metropolis algorithm) one gets in this case $\nu = 0.6327(20)$, $\beta = 0.3273(17)$, and $z = 2.042(6)$.

The advantage of the short-time dynamic approach compared to simulations in equilibrium is that is free of critical slowing down since the spatial correlation length is small within the time regime, even at or near the critical point. Thus in case of local algorithms (Metropolis, heatbath) the CPU time to get

8

comparable results for different systems is independent of the system size, while simulations in the long-time regime suffer from critical slowing down. However, if we use the HMC algorithm increasing the system size leads also for simulations in the short-time regime to an increase of the CPU time since we have to scale the step size $\Delta t'$. Therefore, determing the static critical exponents can be done easier if we use local algorithms (and short-time dynamics). However, if one wants to measure the dynamic critical exponent z or include fermions in the simulation one has to use the HMC algorithm. In this case using the dynamic relaxation is advantageous compared to conventional simulations in equilibrium.

6 Summary and conclusions

We presented comprehensive Monte Carlo simulations of the short-time critical dynamics for SU(2) lattice gauge theory in $(3+1)$ dimensions. The dynamics of the system was given by the HMC algorithm. Starting from the ordered state, the magnetization (Polyakov loop), its derivative with respect to the coupling constant and the cumulant were measured at the critical point. The observables obey a power law behaviour after some microscopic time scale t_{mic} as expected. The critical exponents $\beta/\nu z$, $1/\nu z$ and d/z are determined from these time dependencies. The results support a universal short-time scaling behaviour for SU(2) gauge theory in $(3+1)$ dimensions. The values for the static exponents β and ν agree within statistical errors with those measured in equilibrium and with those of the three-dimensional Ising model. Thus the $(3+1)$-dimensional SU(2) lattice gauge theory and the Ising model in three dimensions are in the same universality class. The dynamic critical exponent for the HMC algorithm was determined with $z = 2.0(1)$. The work could extended to SU(2) lattice gauge theory with dynamical fermions.

References

[1] H.K. Janssen, B. Schaub, B. Schmittmann, Z. Phys. B 73 (1989) 539.

[2] P.C. Hohenberg, B.I. Halperin, Rev. Mod. Phys. 49 (1977) 435.

[3] A review of short-time dynamics is given in: B. Zheng, Int. J. Mod. Phys. B 12 (1998) 1419.

[4] Z.B. Li, L. Schülke, B. Zheng, Phys. Rev. Lett. 74 (1995) 3396.

[5] Z.B. Li, L. Schülke, B. Zheng, Phys. Rev. E 53 (1996) 2940.

[6] L. Schülke, B. Zheng, Phys. Lett. A 215 (1996) 81.

[7] A. Jaster, J. Mainville, L. Schülke, B. Zheng, J. Phys. A: Math. Gen. 32 (1999) 1395.

[8] A. Jaster, Phys. Lett. A 258 (1999) 59.

[9] A. Jaster, Phys. Lett. A 258 (1999) 177.

[10] H.J. Luo, L. Schülke, B. Zheng, Phys. Rev. Lett. 81 (1998) 180; Phys. Rev. E 57 (1998) 1327.

[11] H.P. Ying, H.J. Luo, L. Schülke, B. Zheng, Mod. Phys. Lett. B 12 (1999) 1237.

[12] K. Okano, L. Schülke, B. Zheng, Phys. Rev. D 57 (1998) 1411.

[13] S. Duane, A. Kennedy, B. Pendleton, D. Roweth, Phys. Lett. B 195 (1987) 216.

[14] J. Engels, J. Fingberg, M. Weber, Nucl. Phys. B 332 (1990) 737; J. Engels, J. Fingberg, D.E. Miller, Nucl. Phys. B 387 (1992) 501; J. Engels, J. Fingberg, V.K. Mitrjushkin, Phys. Lett. B 298 (1993) 154; J. Engels, S. Mashkevich, T. Scheideler, G. Zinovjev, Phys. Lett. B 365 (1996) 219.

[15] B. Svetitsky, G. Yaffe, Nucl. Phys. B 210 [FS6] (1982) 423.

[16] K. Jansen, C. Liu, Nucl. Phys. B 453 (1995) 375; B 459 (1996) 437; C. Liu, A. Jaster, K. Jansen, Nucl. Phys. B 524 (1998) 603.
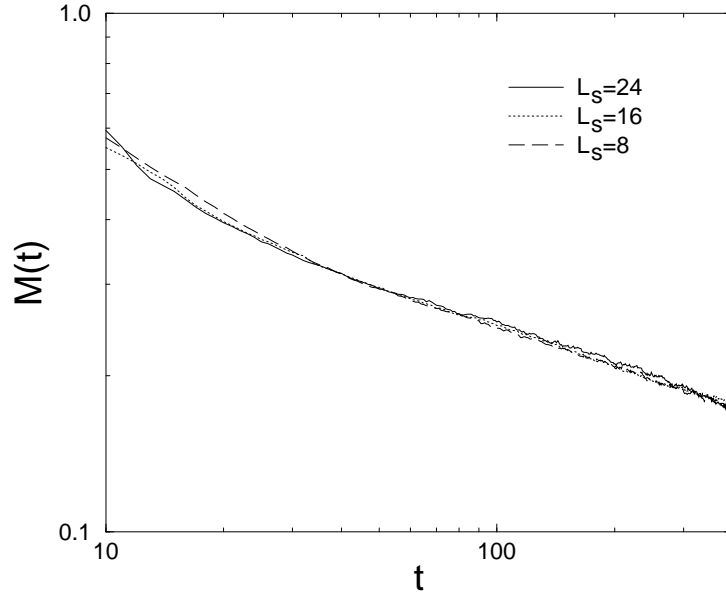
[17] T. Lippert, preprint hep-lat/9712019.

Fig. 1. Time evolution of the magnetization at the critical point starting from the ordered state for $L_s = 8$, 16 and 24. The length of a trajectory of a HMC step was $t' = 0.32$ with $N_{MD} = 80$ intermediate points.
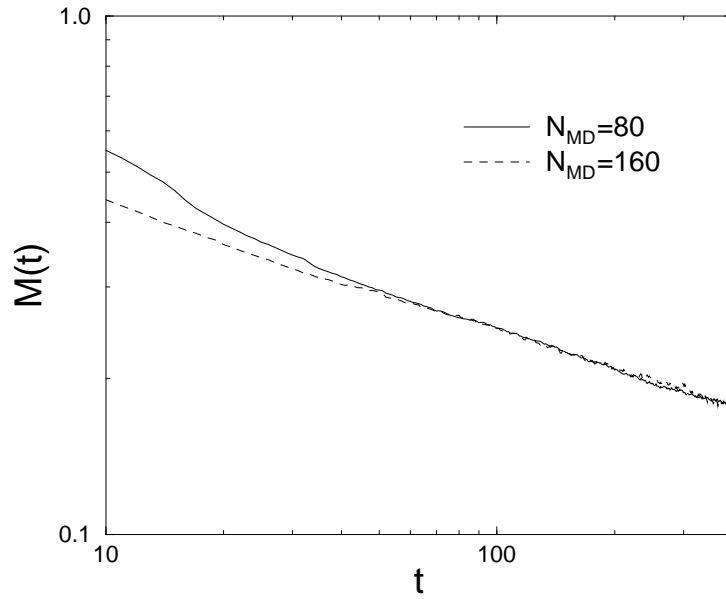

Fig. 2. Magnetization as a function of time for $L_s = 16$ and $t' = 0.32$ at the critical point. A trajectory consists of $N_{MD} = 80$ steps in the first case (full line) and $N_{MD} = 160$ steps in the second case (dashed line).

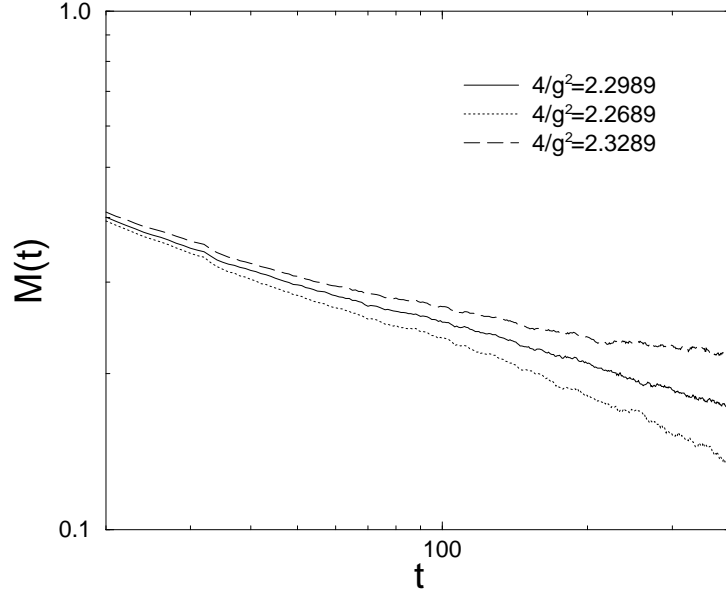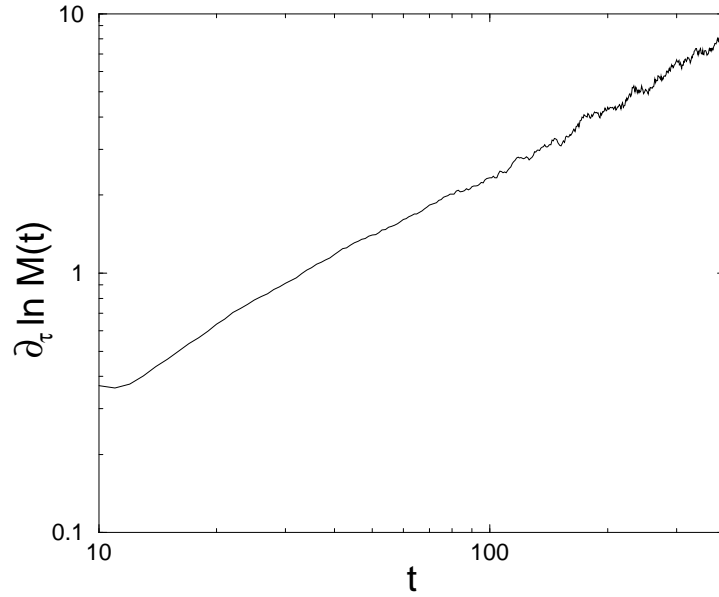Fig. 3. Time evolution of the magnetization for three values of the coupling constant with $L_{\mathrm{s}} = 16$ and $N_{\mathrm{MD}} = 80$.

Fig. 4. Logarithmic derivative of the magnetization with respect to τ taken at g_{c}, obtained from the curves shown in Fig 3.